Jasmin Kirsch, Kim Sina Reinauer, Heike Meissner, Martin Dannemann, Michael Kucher, Niels Modler, Christian Hannig, Marie-Theres Weber

Ultrasonic and sonic irrigant activation in endodontics: A fractographic examination

Introduction: The aim of the present study was to assess the failure mode of current sonic (EndoActivator, Dentsply Maillefer, Ballaigues, Switzerland; Eddy, VDW GmbH, Germany) and ultrasonic (Irri S, VDW GmbH, Germany, Endo Soft Intruments EMS, Nyon, Switzerland) tips in artificial and standardized root canals with different, representative radii of curvature.
Materials and Methods: 100 extracted human lower first and second molars were examined with regard to their 5 most common radii of curvature (2.5/ 3/ 6/ 9/ 11 mm) and the mean length of their root canals. In addition, a straight canal was chosen and served as control. The canals were milled into an artificial steel model. The cyclic fatigue testing took place with the Tiratest 2720 at 120 mm/min. Every file was tested for 12 min (8 cycles). A fractographic examination took place with a scanning electron microscope.
Results: All tested Irri-S instruments fractured in the canal with a 2.5 mm radius of curvature, 70 % of the IrriS fractured in the canal with a 3 mm radius of curvature. The ESI, EDDY and EndoActivator tips showed no fracture ($p < 0.05$), but surface wear and erosion of the instrument tips were visible. In addition, ESI and EndoActivator showed no signs of cavitation.
Conclusions: There is no existing irrigation activation system that provides surface quality of the tip and cleaning efficiency of the canal. Especially, in canals with a small radius of curvature the use of EDDY may be a safe advice.

Keywords: sonic application; ultrasonic application; root canal irrigation; curvature radius

Clinic of Operative Dentistry, Medical Faculty Carl Gustav Carus, TU Dresden: Jasmin Kirsch, Kim Sina Reinauer, Heike Meissner, Prof. Dr. Christian Hannig, Dr. Marie-Theres Weber
Technische Universität Dresden, Institute of Lightweight Engineering and Polymer Technology (ILK), Faculty of Mechanical Engineering: Dr. Martin Dannemann, Michael Kucher, Prof. Dr. Niels Modler
Citation: Kirsch J, Reinauer KS, Meissner H, Dannemann M, Kucher M, Modler N, Hannig C, Weber M-T: Ultrasonic and sonic irrigant activation in endodontics: A fractographic examination. Dtsch Zahnärztl Z Int 2019; 1: 209–221
Peer-reviewed article: submitted: 12.05.2019, revised version accepted: 27.06.2019
DOI.org/10.3238/dzz-int.2019.0209–0221

Introduction

Effective irrigation is a key factor for a successful root canal treatment. Thereby, the removal of the smear layer, remaining pulp tissue, bacteria and their endotoxins and decomposition products is essential for the endodontic success [2, 44, 53]. As a result, a reduction of bacteria can be achieved with a factor of 100–1000.

It has been known for years, that due to the difficult canal anatomy it is impossible to shape and clean the root canal system completely [6, 13, 17, 18, 21, 23–25, 43, 46, 49]. Therefore, chemical agents serve as irrigating solutions to clean untouched areas such as isthmi, dentinal tubules and complex apical structures [22, 46]. However, it is difficult to transport the irrigant to these specific areas, especially in the apical portion of the canal [21]. Previous studies have shown that sonic or ultrasonic activation of the irrigating solution can improve the agents' positive properties. In the past years, ultrasonic and sonic activation systems have been extensively examined [5, 15, 16, 20–22, 29–31, 33, 38, 45, 51]. Unfortunately, there are unpredictable treatment situations where activation tips fracture [32]. Especially, the fracture of the expensive ultrasonic irrigant activation tips result in complicated treatment situations. The removal of the fractured file cannot be guaranteed in all treatment cases. In the worst case, that scenario leads to the loss of the tooth and the failure of the root canal treatment. Screening the literature to our best knowledge, there is no study that determines the failure mode of irrigation activation devices.

To examine failure modes of sonic and ultrasonic tips, basic knowledge is necessary. Several parameters such as experience and performance of the dentist, the quality of the intraradicular dentin, the taper after root canal treatment, the curvature radius of the root, the material and the geometry of the irrigant activation tips influence the fracture characteristics of these tips. However, in order to achieve reproducible results with low scattering of the measurement values, a standardized model with few variables has been introduced in the present study. Hereby, the influencing parameters dentist, dentin and taper were substituted by constant parameters. The primary focus of the study was therefore the root canal curvature radius and its impact on the irrigation tips. Using the identical application mode, the reproducible failure of the tips was tested under standardized conditions.

The aim of this study was therefore to assess the failure mode of current sonic and ultrasonic tips in artificial and standardized root canals with different, representative radii of curvature.

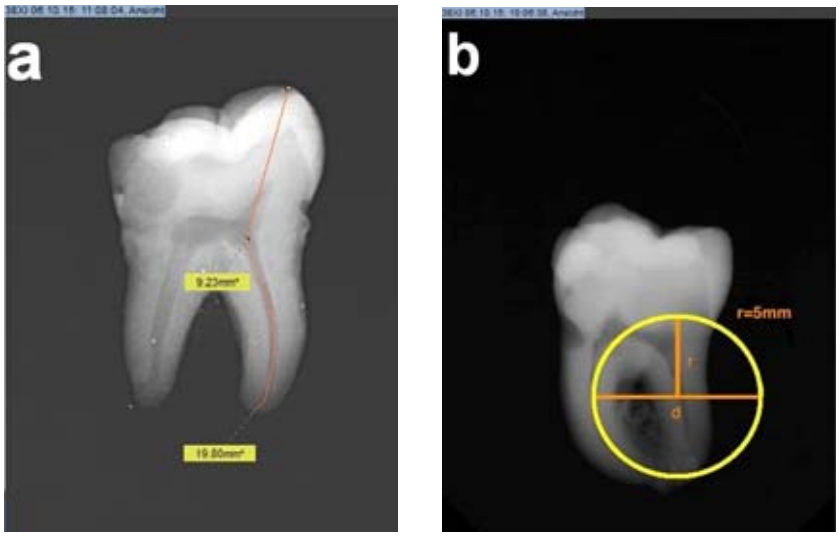

(Fig. 1, 2 and 6: Kim Sina Reinauer)

Figure 1a–b Exemplary measured teeth by means of the X-ray program Sidexis (Heliodent Plus, Sirona, Germany). The depth of the access cavity (in the present example: 9.23 mm) and the root canal length (19.8 mm) were measured (**a**). In addition, the radius of curvature of the left distal canal was calculated (in the present example: 5 mm) by applying a various radius over the entire length of the distal root canal (**b**).

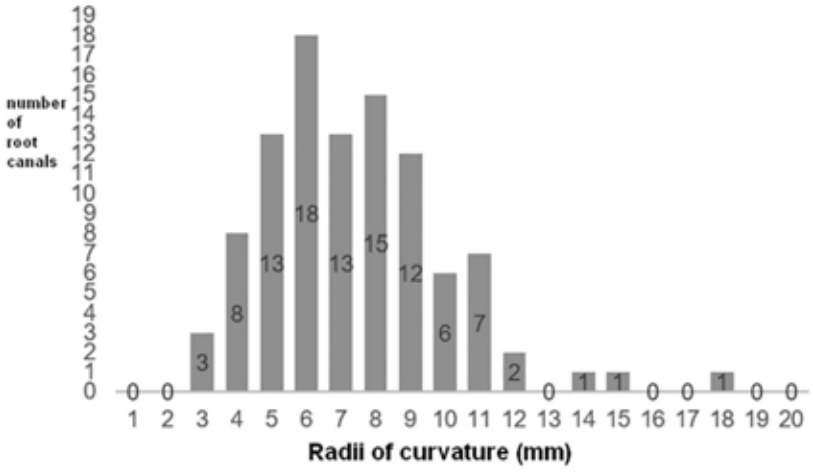

Figure 2 Distribution of the radius of curvature found in 100 lower molars' distal canals. The 3 mm radius of curvature was the smallest radius, which was found in the present radiographic examination, 6 mm was the most common radius of curvature and 8 mm was the second most common radius of curvature. In addition, an 11 mm radius of curvature was exemplary chosen to represent a large radius of curvature.

Material and Methods

Prestudy

100 extracted human lower first and second molars of middle-aged donors were extracted during routine sur-

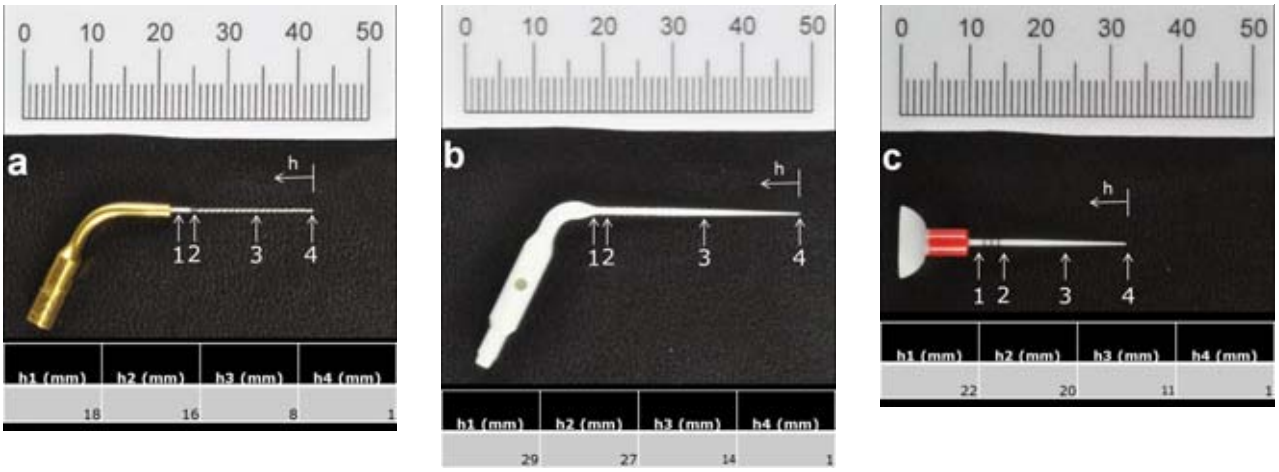

(Fig. 3 and 5: Michael Kucher)

Figure 3a–c The sonic and ultrasonic tips (a–c) were measured by an electronic outside micrometer to define the parameters (maximum and minimum diameter) for the artificial steel model. The diameter was measured in different spots (h1–h4; **a–c**). Every spot was measured 10 times. For the construction of the root canal model, the maximum diameter was determined. Thereby, the diameter measurement was conducted for the IRRI S ultrasonic tip (**a**), the Eddy sonic tip (**b**) and the EndoActivator sonic tip (**c**).

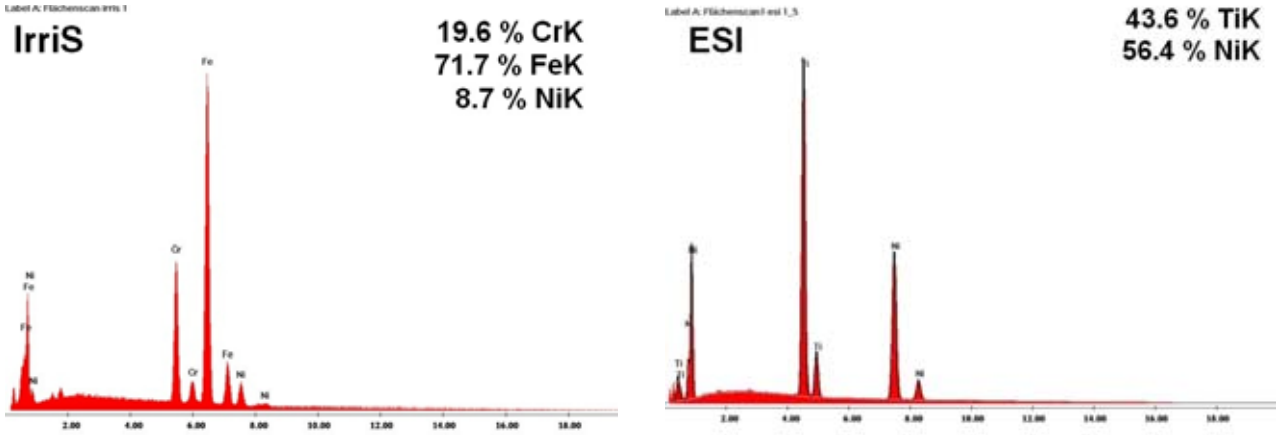

(Fig. 4 and 7–15: Heike Meissner)

element	weight percentage %
CrK	19.6
FeK	71.7
NiK	8.7
total	100

element	weight percentage %
TiK	43.6
NiK	56.4
total	100

Figure 4 Results of the Energy-dispersive X-ray spectroscopy (EDX) analysis of Irri S and ESI tips: The material composition was detected and showed that the Irri S consists of chromium, iron and nickel. In contrast, the ESI tip consists of nickel and titanium.

gical treatment in the department of maxillo-facial surgery. The teeth were stored in thymol solution at 4 C and analyzed by means of root canal curvature regarding the distal canal. Inclusion criteria for the study were: lower first and second molar, C-(entirely curved) and J-(apical curve) [34] shaped configuration of the molars' distal canal and an intact apex. Exclusion criteria were calcifications, previous root canal treatment, fractures, resorptions, S-(multicurved) and I-(straight) shaped configuration of the molars' distal root canal [34]. Hereby, 2-dimensional and orthograde radiographic visualization took place (Heliodent Plus, Sirona, Germany) (Fig. 1a). The aim of the chosen method was to facilitate the selection process of the included teeth.

Artificial root canal model

The teeth were measured by the x-ray program Sidexis (Heliodent Plus, Sirona, Germany). First, the depth of

the access cavity (distance between the reference cusp and root canal orifice) as well as the root canal length (distance between canal orifice and root canal apex) was determined (Fig. 1a). This calculation resulted in an average access cavity depth of 11 mm and an average root canal length of 9 mm. Consequently, an average total length of 20 mm was obtained for the standardized model (Fig. 2). Second, the radius of the distal canal curvature was calculated (Fig. 1b). Thereby, the radius of curvature was measured by approximating the distal root canal's curved section using a circle with varying radius. Different curvatures are represented by the size of the radius. A large radius stands for a small curvature and a small radius represents a strong curvature. Regarding the frequency of distribution, the statistical analysis was performed by the statistic program SPSS. Hereby, the mean values of the total root canal length, the depth of the access cavities as well as the radius of the curvature were calculated.

The following radii of curvature were chosen for the artificial root canal model (Fig. 2):

- 2.5 mm: this configuration was not detectable in the x-rays, it was chosen to test the load limit
- 3 mm: smallest radius of curvature
- 6 mm: most common radius of curvature
- 8 mm: second most common radius of curvature
- 11 mm: exemplary for a large radius of curvature
- R: representing a straight canal

In the following, the diameters of the sonic and ultrasonic tips were measured by an electronic outside micrometer (Holex, Hoffmann group, Munich, Germany). Thereby, the measuring range was between 0–25 mm, the accuracy was within 0.001 mm and the width of the stamp was 6 mm. The sonic and ultrasonic tips were measured in different spots and the maximum diameter was calculated for every position (Fig. 3 a-c). The measurement revealed a large range in diameter between the sonic and ultrasonic files. For this reason, 2 different test series were created for sonic (diameter: 1.2 mm) and ultrasonic files (diameter: 0.8 mm) (Fig. 5 and 6). The diameter of these artificial root canals was designed to fit the files in their oscillating mode and represent a curved root canal. Therefore, the size was created 4 ISO-sizes larger than the average original diameter of the sonic (maximum diameter: 1 mm) and ultrasonic (maximum diameter: 0.6 mm) files.

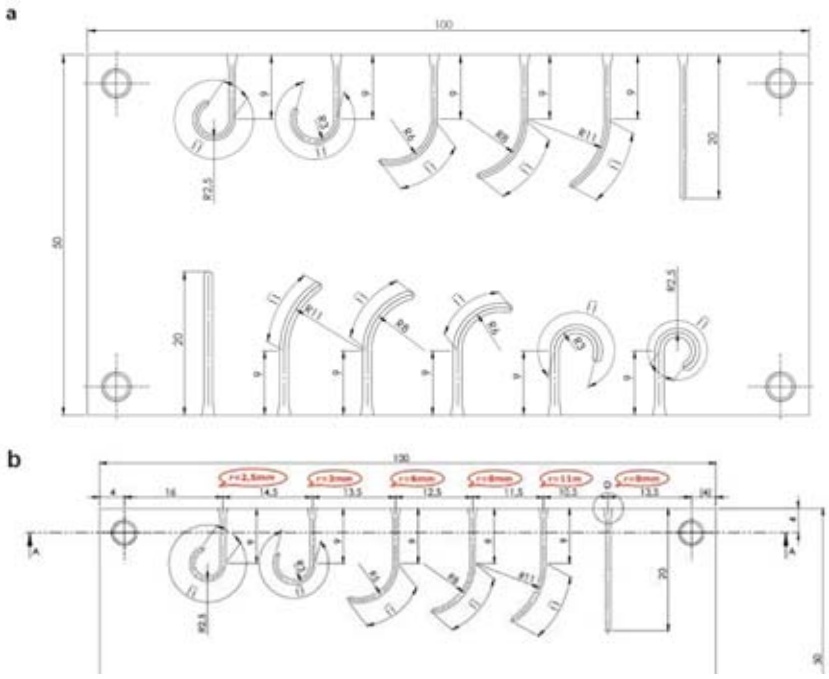

Figure 5a–b Design drawing of the root canal model. With the results of the diameter and radius of curvature measurements, a root canal model was obtained (**a–b**). The arc length of the artificial root canals was always defined at 20 mm, the root canal diameter at 0.8 mm for ultrasonic files (**b**) and 1.2 mm for sonic files (**a**; lower row).

With the acquired information, a root canal model was obtained (Fig. 5 and 6). The present study included a steel model (Fig. 6) with C- and J-shaped root canal configurations differing in the most distributed curvature radii calculated earlier by statistical analysis (Fig. 2). The artificial root canals had always the same access cavity and root canal's arc length (20 mm). The square cross-section throughout the root canals had an inner dimension of 0.8 mm for ultrasonic files and 1.2 mm for sonic files (Fig. 5 and 6).

Irrigation procedure

The cyclic fatigue testing took place with the Tiratest 2720 (Tira GmbH, Schalkau, Germany) at 120 mm/min with the following sonic and ultrasonic activation tips (Fig. 6b). The tips are driven in each case by means of the manufacturer's original tool holder. The stress of the irrigation tip results of the bending deformation during the penetration and the additional dynamic stress due to sonic and ultrasonic oscillations.

Sonic tips

EndoActivator (EA) group, (Dentsply Maillefer, Ballaigues, Switzerland), with a size 25, 4 % taper tip, 22 mm length, placed at working length (WL) –1 mm (n = 10 tips per tested radius of curvature).

Eddy (ED) group, (VDW, Munich, Germany), with a size 20, 2 % taper tip, 28 mm length, mounted on a scaler (Pferdefit Dental, Hohenstein-Breithardt, Germany). Tip placement and irrigation/activation times were identical to the EA group (n = 0 tips per tested radius of curvature).

Ultrasonic tips

In addition, Energy-dispersive X-ray spectroscopy (EDX) analysis of Irri S and ESI tips was carried out with an XL 30 ESEM (Philips, Eindhoven, The Netherlands) with an EDX system

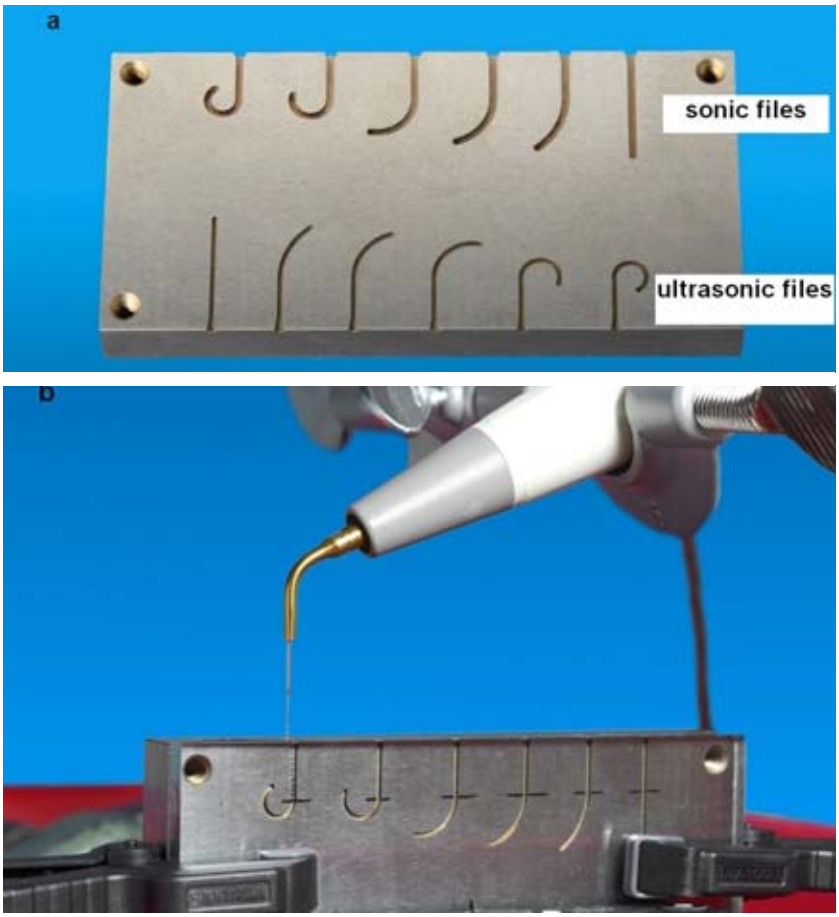

Figure 6a–b Figure 6 shows the obtained artificial steel root canal model for the testing of sonic files (**a**, 1.2 mm diameter, upper row) and ultrasonic files (**a**, 0.8 mm diameter, lower row). The cyclic fatigue testing took place with the Tiratest 2720 at 120 mm/min (**b**). The starting point was placed at the canal orifice at 9 mm (**b**, marked line). The file penetrated 10 mm into the canal and stopped 1 mm before reaching the apex to ensure the working length (19 mm).

(Phoenix, EDAX INC., Mahwah, N.J., USA) in order to detect the material composition of the 2 tips (Fig. 4).

Irri S, (Ultrasonic irrigant activation Group, VDW GmbH, Germany), with a size 20 tip, 0.3 % taper, 21 mm length, mounted on an ultrasonic unit (VDW Ultra, VDW GmbH, Germany) at a power setting of 30 % according to manufacturer's settings. Tip placement and irrigation/activation times were identical to the EA and Eddy groups (n = 10 tips per tested radius of curvature).

ESI, (Endo Soft Instruments EMS, Nyon, Switzerland), with a size 15 tip, 0,3 % taper, 22 mm length, tip placement and irrigation/activation times were identical to the EA, Eddy and Ultrasonic irrigant activation groups (n = 10 tips per tested radius of curvature).

After every cycle, a rinsing with water took place. Every file was tested for a total time of 12 min (representing 90 s for each of the 8 cycles). The starting point was placed at the canal orifice at 9 mm, clinically at the beginning of the root canal. When starting, the file penetrated 10 mm into the canal (Fig. 6b) and stopped 1 mm before the apex to ensure the whole working length.

During the irrigation procedure, a microscopic camera at a resolution of 2560 x 2048 pixel and a frame rate of 30 frames/second detected the presence of long-time cavitation phenomena for every tested tip.

Inspection of the instruments and fractographic examination

The instrument tips were autoclaved and then ultrasonically cleaned in absolute alcohol prior to scanning electron microscopic examination (SEM, XL 30 ESEM, Philips, Eindhoven, The Netherlands) as described earlier [8]. At different views, images of the fractured surface were obtained at high magnifications. Two examiners examined the fractographic images. Thereby, fatigue striations which are characteristic for metallic materials [8] were detected for the Irri S and ESI instrument tips.

According to Collins, the 4 recognized modes of fracture in metal [9, 10] were used to categorize the present failure mode of the Irri S and ESI tips:

1. Cleavage: "Refers to the cracking of a crystalline solid along slip planes" [8].
2. Dimple rupture: "The typical fractographic appearance of ductile failure; under (tensile or shear) load internal voids (due to inclusions, microporosities, precipitates or other microstructural heterogeneities) grow in size until the remaining material in between these 'holes' fails because of overload" [11].
3. Fatigue: "A form of transgranular fracture where the grain boundaries have little effect on the direction of crack propagation" [8, 41].
4. Decohesion: "The rupture of a material along grain boundaries, usually under the influence of environmental factors, such as hydrogen embrittlement or attack by corrosive agents"[11].

The mechanisms of fatigue [7, 47] and fatigue crack growth [36, 39] of polymeric materials are based on the general modes established for metals [7]. Interestingly, both materials show similar stress-life curves and fatigue crack growth curves [7]. Therefore, the fractographic examination of the Eddy and EndoActivator tips was carried out in a similar manner according to the failure modes of Irri S and ESI tips. In addition, the distance between the fractured ends and the tips of the instruments were measured to calculate the length of the fractured segment for each instrument.

In order to calculate the development of the failure intensity, the following steps were performed:

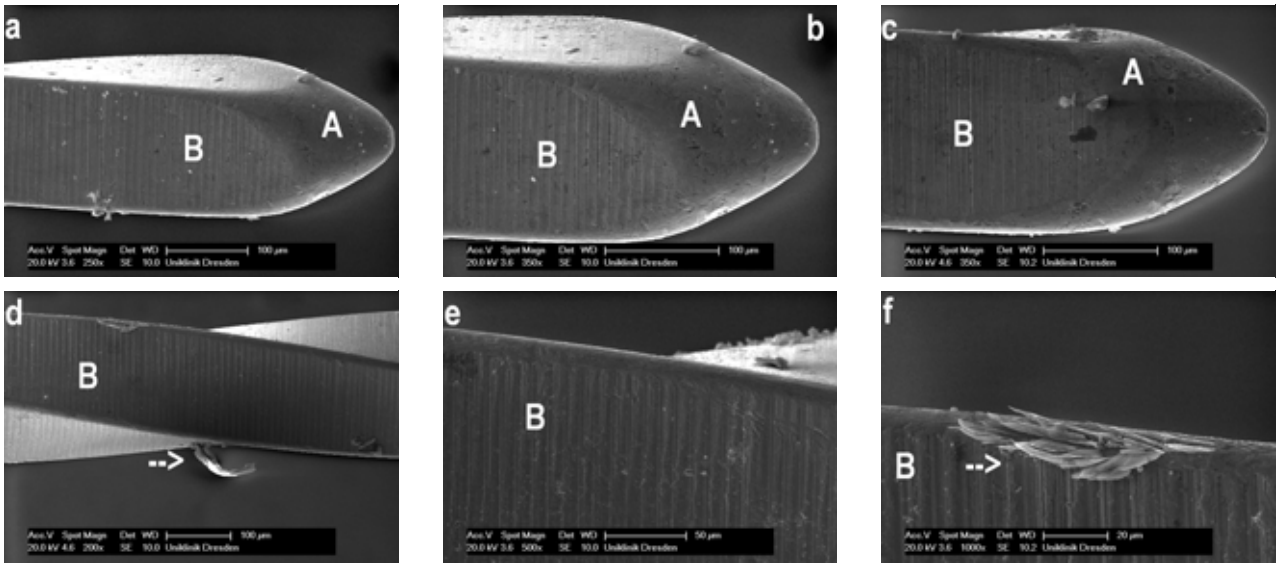

Figure 7a–f Initial state of the Irri S instrument tip: Instrument surface showing no surface wear (**a–c**; A) but manufacturer-dependent material characteristics (**a–f**; B). In addition, fanned out areas were detected at the material surface (**d, f**; arrow).

A) No surface wear
B) Manufacturer-dependent material characteristics
Arrow: Fanning out of the material surface

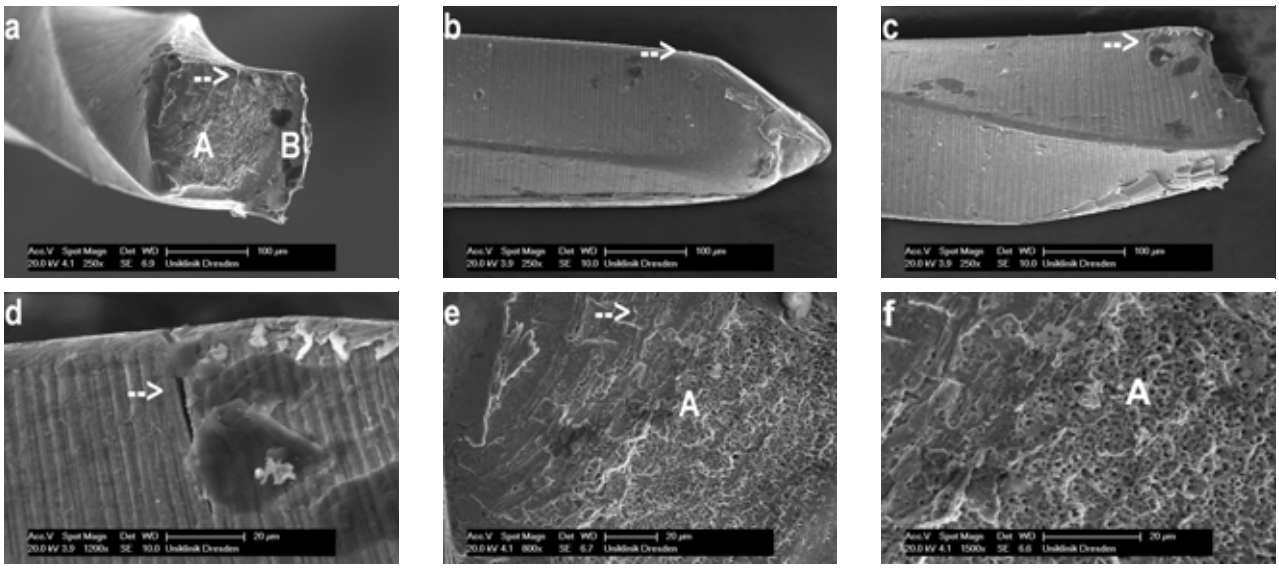

Figure 8a–f Fracture surface of an Irri S tip (**a, e, f**) showing fatigue striations, crack initiations (arrows) and areas not involved in fatigue striations (**a**; B). The profile of the tip reveals the presence of further crack initiations at the periphery of the instrument (**b, c, d**; arrows). Note the areas with skewed dimples on high power view (**f**; A).

A) Skewed dimples
B) Areas not involved in fatigue-crack propagation
Arrow: Crack initiation

- Evaluation of the failures, failure frequency and failure intensity
- Evaluation of the differences between the different sides of each tip (numerical – by calculating the 4 sides) coefficient of variation (mean squared deviation, referred to the mean value) of the mean failure intensity respectively to the number of failures.

Data analysis

Statistical analysis was performed by Anova ($\alpha = 0.05$) and Bonferroni holm correction ($p = 0.01$) using SPSS 22.0 software (SPSS, IBM, Germany). In the present study, the following null hypothesis is tested: No fractures of the sonic and ultrasonic tips occur in the different shaped canals.

Results

The analysis of the radii of curvature demonstrated that the 3 mm radius

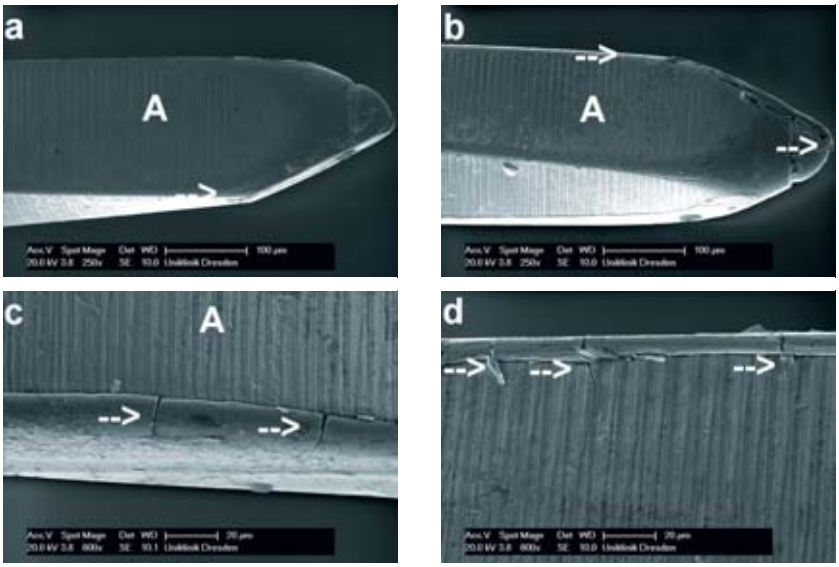

Figure 9a–d Irri S tip showing signs of crack initiation at the periphery of the instrument without the fracture of the tip (**a–d**; arrow). Presence of manufacturer dependent material characteristics on the surface of the instrument (A).

A) Manufacturer-dependent material characteristics
Arrow: Crack initiation

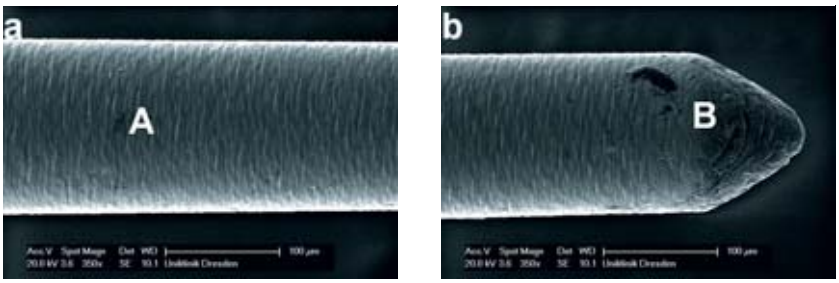

Figure 10a–b Initial state of the ESI-instrument tip: Instrument surface showing no surface wear (**a**; A) but manufacturer-dependent material characteristics (**b**; B).

A) No surface wear
B) Manufacturer-dependent material characteristics

of curvature was the smallest radius, which was found in the present radiographic examination (3 teeth) of 100 lower molars' distal canals examined. A 6 mm radius of curvature was the most common radius (18 teeth), followed by 8 mm, the second most common radius of curvature (15 teeth, Fig. 2). In addition, an 11 mm radius of curvature was exemplary chosen to represent a large radius of curvature (7 teeth, Fig. 2).

The results of the Energy-dispersive X-ray spectroscopy (EDX) analysis of Irri S and ESI tips showed that the Irri S consists of chromium, iron and nickel. In contrast, the ESI tip consists of nickel and titanium.

As determined by Anova and Bonferroni tests, there were significant differences ($p < 0.01$) between the tested instrument tips. Thereby, all Irri S tips fractured in the 2.5 mm radius canal (n = 10) and 70 % of the Irri S tips fractured in the 3 mm radius canal (n = 10). All other tested systems achieved significant better results, since there were no fractures of the EDDY-, EndoActivator- and ESI-tips in the examined canals with different radii of curvature.

A pre-inspection of the Irri S tips showed that these tips displayed more surface defects on the surface than the other tested tips. These defects were unevenly distributed on the 4 surfaces of the instrument and concentrated on the tips edges. Therefore, the inspection and examination of the instruments had to take place in 4 directions (each rotation around 90°).

At high magnification of the initial state of the Irri S instrument tip, the surface showed manufacturer-dependent material characteristics (Fig. 7) with fanned out areas (Fig. 7d, f). In all cases (n = 10; 100 %) the fracture surface of the Irri S tips showed fatigue striations (Fig. 8) after application of the tip into the 2.5 mm radius of curvature canal. These fatigue striations indicate a fatigue failure mode. After the application into the 3 mm radius of curvature canal, 7 cases (70 %) showed fractured Irri S tips. In lateral view, further crack initiations at the periphery of the instrument (Fig. 8c–d) as well as skewed dimples in areas not involved in fatigue crack initiation were visible (Fig. 8e–f). Further, Irri S tips without fracture of the tip showed crack initiations at the periphery of the instrument (Fig. 9a–d, arrow). The mean length of the fractured segments was 7.9 mm ± 2.2 mm in the 2.5 mm radius-canal and 7.2 mm ± 2 mm in the 3 mm radius-canal measured from the tip's free end. At the edges of the Irri S tip's deformation areas, many transverse cracks were observed. Subsequently, further material spalling is possible. Furthermore, these massive and irregular edge deformations were also detectable in the unfractured Irri S tips.

The microscopic analysis of the ESI-instrument tip surface also showed manufacturer-dependent material characteristics in the initial state (Fig. 10b). In contrast to the other tested tips, this series (NiTiAl-material) displayed a cylindrically symmetric, non-angle shaped form and the surfaces showed lower machining grooves. Only the taper surfaces had noticeable process-induced transverse grooves. After the usage of the tip, low surface wear and a levelled surface relief with scratches, material abrasion and an erosion of the instrument tip were visible (Fig. 11a–d). The different radii of curvature had almost no impact on the fracture pattern and frequency.

The surfaces of the EDDY and EndoActivator instrument tips also showed manufacturer-dependent material characteristics (Fig. 12 and 14). Thereby, polymer structures were detectable at the tip of the Eddy instrument (Fig. 12a–c) and at the synthetic joint of the EndoActivator (Fig. 14 a, c–f). After Application of these 2 sonic activation devices, surface wear, a levelled surface relief and material abrasion were visible (Fig. 13 and 15).

All Eddy activation tips displayed a casting seam caused by the casting of the polymer material. Throughout the experiments, this casting seam was exposed to particular stress and showed cracks and spalling. The first SEM images were taken with 20 keV primary energy. Thereby, higher magnification (2000x and higher) caused defects in the material (porosities, cracks). Consequently, all the SEM images which were analyzed in the present study were taken with 5 keV primary energy. Thereby, all EDDY samples displayed a strong erosion of the instrument tip (Fig. 13a–c). On the surface of the blunt EndoActivator tip a lower erosion of the instrument tip was visible, too (Fig. 15a–b). Besides, crack initiation at the periphery of the instrument was detectable (Fig. 15c, arrow). The examination with the microscopic camera showed cavitation of the Irri S tip and Eddy tip but no signs of cavitation for the ESI and EndoActivator tips.

Discussion

The removal of bacteria and their endotoxins from the complex root canal system is one of the goals of root canal therapy. Different strategies such as delivery or irrigant activation systems can enhance the effect of the disinfection procedure. Thus, practitioner can safely use these helpful techniques, it is necessary to ensure a certain user and patient safety. Therefore, the aim of the present in vitro study was to evaluate

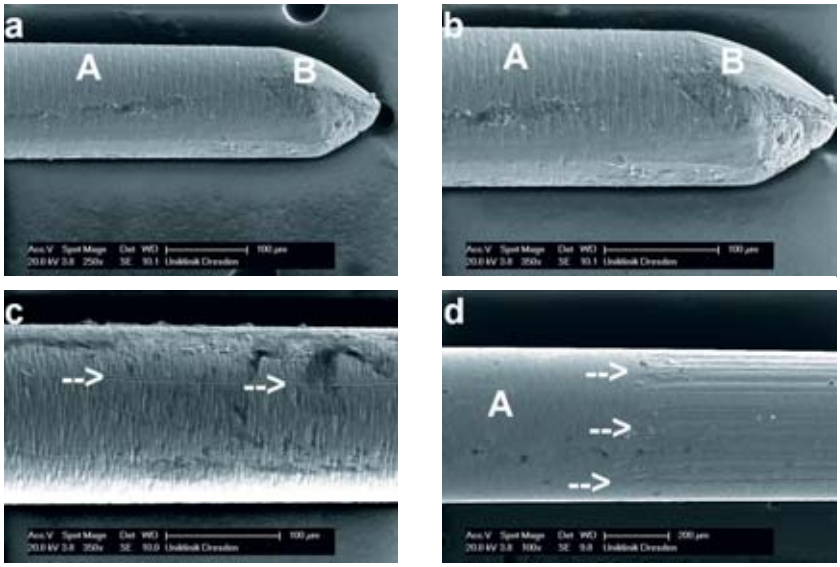

Figure 11a–d ESI-tip showing no signs of fracture or crack initiation at the periphery of the instrument. Although, low surface wear (**a, b, d**; A) and a levelled surface relief (**a–b**; B) with scratches, material abrasion (**c**; arrow) and erosion of the instrument tip are visible (**a–b**; B).

A) Low surface wear
B) Levelled surface relief and erosion of the instrument tip
Arrow: Scratches and material abrasion

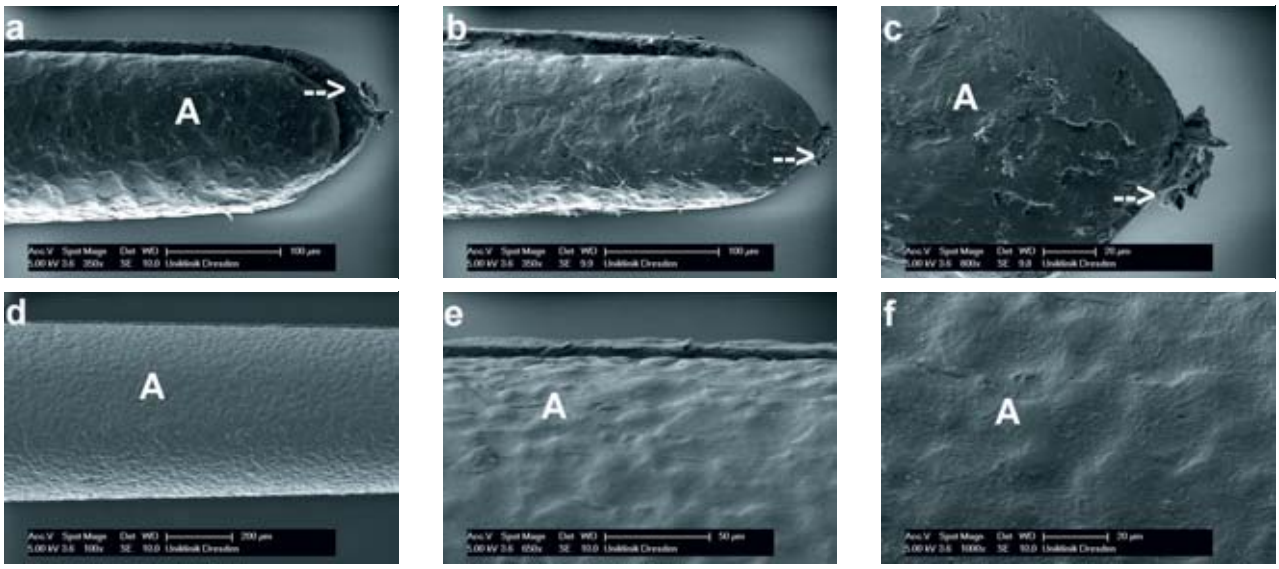

Figure 12a–f Initial state of the Eddy-instrument tip: Instrument surface showing no surface wear but manufacturer-dependent material characteristics like adhesion of polymer structures at the tip of the instrument (**a–c**; arrow) and a structured surface (**a, c, d, e, f**; A).

A) Manufacturer-dependent material characteristics
Arrow: polymer structure adhesion

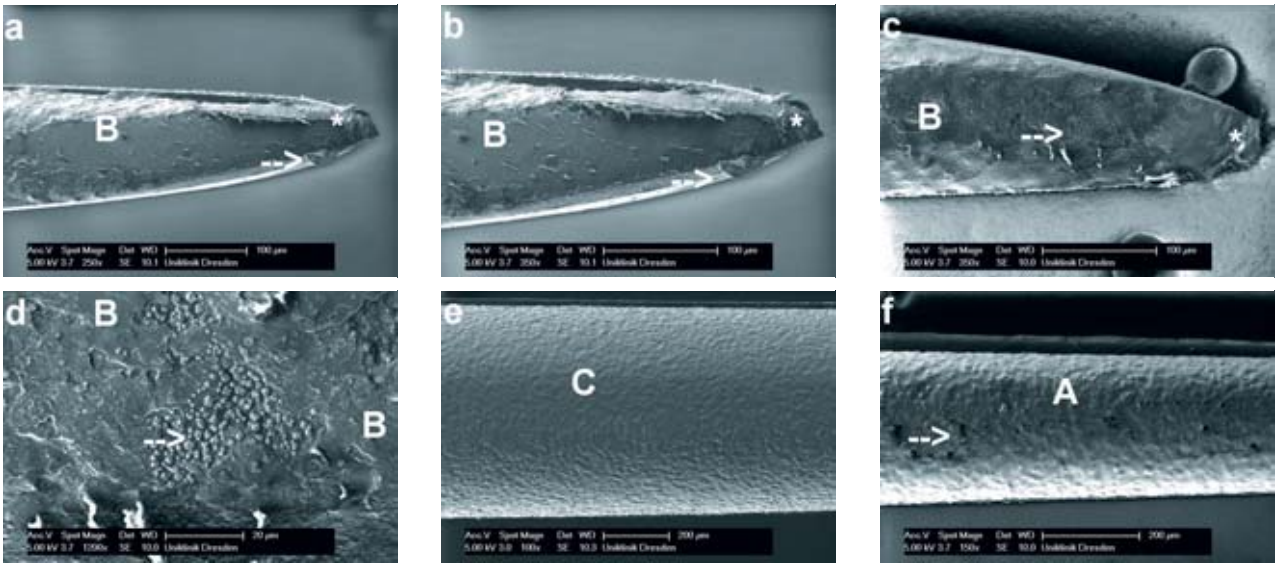

Figure 13a–f Eddy tip showing no signs of fracture or crack initiation at the periphery of the instrument. Although, surface wear (**a–d, f**; A) and a levelled surface relief (**a–d**; B) with scratches (**a–b, f**; arrow), material abrasion (**c, d**; arrow) and strong erosion of the instrument tip are visible (**a–c**; *).

A) Surface wear
B) Levelled surface relief
C) Area with low surface wear
* Erosion of the instrument tip
Arrow: scratches (a–b, f) and material abrasion (c–d)

the failure mode of current sonic (EndoActivator, Dentsply Maillefer, Ballaigues, Switzerland; Eddy,VDW GmbH, Germany) and ultrasonic (Irri S, VDW GmbH, Germany, Endo Soft Intruments EMS, Nyon, Switzerland) tips in artificial and standardized root canals with different, representative radii of curvature. The null hypothesis stated that no fractures of the sonic and ultrasonic tips occur in the different shaped canals. However, the results of the present study showed that the null hypothesis can be rejected. The ultrasonic steel tip Irri S fractured in 70 % of the 3 mm radius-canals and in 100 % of the 2.5 mm radius-canals. Although, the 2.5 mm radius represents an extreme curvature, the other tips showed no fracture. This canal configuration might be rare but not uncommon [52].

The radius of curvature, which determines the stress field for the tips, is a more important factor in the susceptibility of the instrument to fracture, than the number of treated root canals as described by Kuhn for bending tests of NiTi rotary files [28]. Thus, in this context, Cheung et al. [8] stated that correct assessment of the root canal curvature cannot be over emphasized. The most common strategy to determine the canal curvature is the method of Schneider [42]. In the present study out of 100 lower first and second molars, merely 2 teeth were suitable to determine the Schneider angle. The reason was the curved canal geometry, which cannot be completely represented by an angle. Since it is not always possible to determine the angle of the curvature by the Schneider method, the Schneider method was rejected and a more important parameter needed to be taken into consideration.

Until now, no study determined the canal curvature using only the radius of curvature as a descriptive parameter of the root canal shape. The use of the radius of curvature specifies the root canal curvature characteristics and therefore improves the standardized representation of the different root canal types in the artificial model. This model is required to obtain an assessment cyclic fatigue of ultrasonic and sonic irrigation activation devices.

In the present study, the curvature radius was measured just from a two-dimensional and facial view. Three-dimensional radiographic imaging like µ-CT would of course improve the analysis of the exact root canal curvature [14]. However, the study of Schäfer et al. [40] showed that 71 % of the distal canals were canals with one curve and S-shaped canals could be found in 18 % of the determined canals (n = 50 first mandibular canals) [40]. As a result, the majority of lower molars dispose one-shaped canals, although this should be manifested in further studies with a greater number of cases. Furthermore, the following requirements for the present artificial and standardized root canal model were selected to meet specific needs.

First, the model was designed to ensure mechanical resistance to the tested sonic and ultrasonic tips. Second, a non-altering surface guaranteed a root canal surface integrity at the beginning and at the end of the examination. The model was therefore manufactured in stainless steel and not with bovine or human dentin, which is very common for cyclic

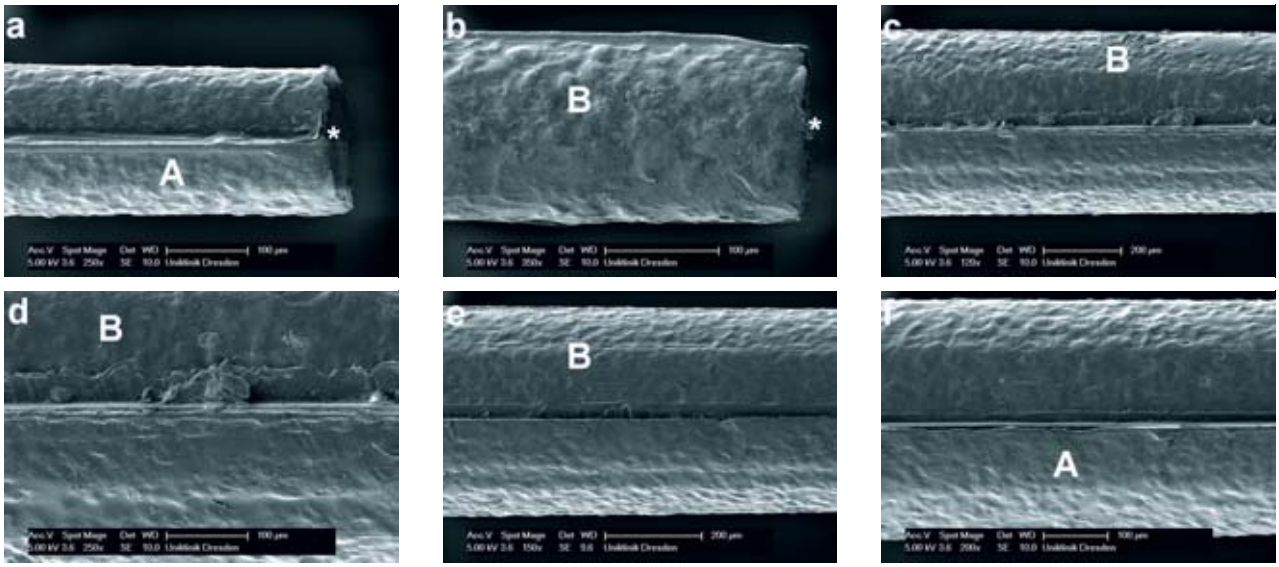

Figure 14a–f Initial state of the EndoActivator-instrument tip: Instrument surface showing no surface wear (**a, f**; A) but manufacturer-dependent material characteristics like the blunt tip (**a–b**; *) and polymer structure adhesion at the synthetic joint (**a, c–f**).

A) No surface wear
B) Manufacturer-dependent material characteristics
* Blunt tip

fatigue resistance testing of endodontic file systems [48]. In laboratory studies, artificial canals have been widely used to evaluate the cyclic fatigue resistance of nickel titanium files to ensure the standardization of experimental conditions [26, 27, 35, 48]. Thereby, stainless steel serves as a stable base material and guarantees identical conditions for the cyclic fatigue testing. Structural differences of the human and bovine dentinal hard tissue (sclerotic dentin, demineralization, amount and density of dentinal tubules) have a potentially high impact on the fracture mode, leading to scattered measurement values. The use of human molars' distal canals was rejected because of the high inter- and intraindividual differences of the root canal geometry, the canal length and the differences in dentin hardness [1, 48]. These unpredictable parameters were excluded in the present study by using a stainless steel model. Furthermore, it should be noted that the square cross-section of the artificial canals is not equivalent to the geometry of human root canals, but it enabled to simulate the almost two-dimensional bending of the endodontic instruments and thus was adapted to examine the failure mode of sonic and ultrasonic tips. However, the results of studies that use artificial canals must be extrapolated to clinical conditions with care because of the differences between a stainless steel block and dentin [4, 48].

As a result the Irri S tip fractured only at the 2.5 mm radius and 3 mm radius canal. The other investigated sonic and ultrasonic irrigant activation devices endured the cyclic fatigue testing procedure but showed, particularly for polymer tips, surface erosion due to interaction with the canals' walls. The reason might be the contact with the stainless steel models' walls. Apparently, the flattening at the edges of the Irri S tip refers to the square diameter of this instrument. It can be assumed, that a high contact pressure is caused by the small contact surface of the tips edges with the artificial root canal. Consequently, the contact pressure exceeds the yield stress of the material and results in plastic deformation. Thereby, the model does not represent a realistic reproduction of the clinical conditions. However, after shaping and rinsing the canal system, it is conceivable that the surface roughness of the dentine can create comparable surface erosions of the polymer tips.

A fractographic examination aims to identify features on the fracture surface that would indicate the origin and the direction of propagation of the cracks leading to material failure (ASM International 1987). According to the classification of Collins [10], the present failure mode was fatigue failure. This failure mode mainly occurs in the area of maximum curvature, particular in small radii, after a certain number of cycles [37]. Starting from an initial crack at the instrument's surface, due to manufacturing defects, repeated plastic deformation enables the crack to propagate and a dimple configuration is created. Once a crack is formed, tension leads to pull the material apart and compression pushes the structure together [8, 50]. With increasing load cycles, these cracks propagate until they reach a critical size and the surrounding material is no longer able to resist the load and the fracture of the ma-

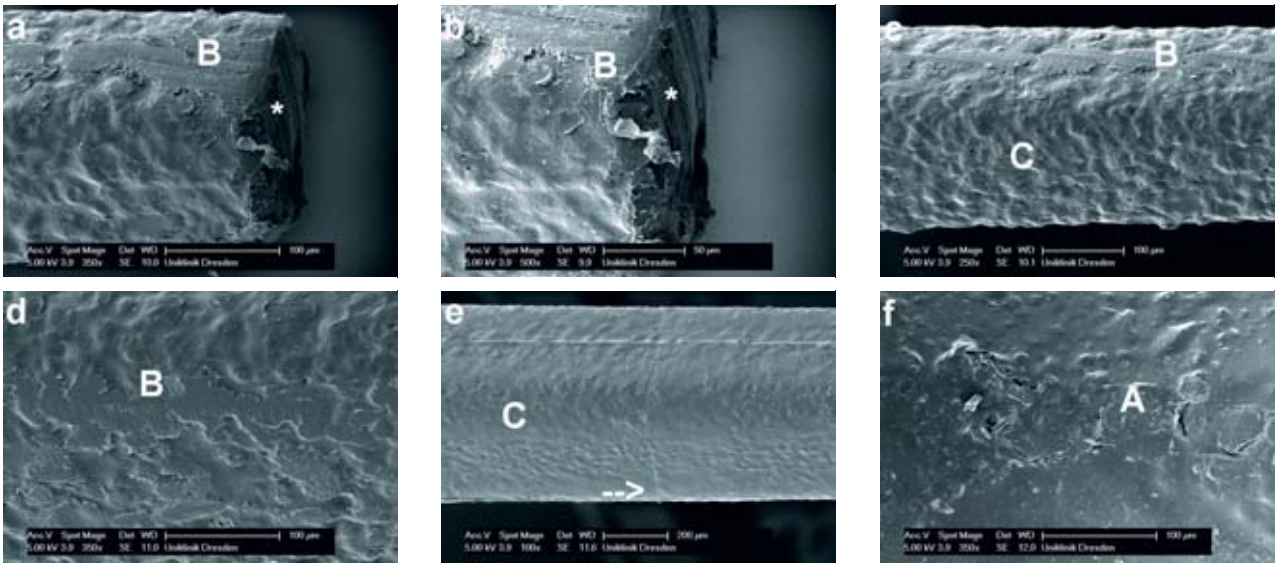

(Fig. 4, and 7–15: Heike Meissner)

Figure 15a–f EndoActivator-tip showing no signs of fracture but crack initiation at the periphery of the instrument (**e**; arrow). Although, surface wear (**f**; A) and a levelled surface relief (**a–d**; B) with erosion of the instrument tip and crack initiation at the periphery of the instrument are visible (**e**; arrow).

A) Surface wear
B) Levelled surface relief
C) Area with low surface wear
* Erosion of the instrument tip
Arrow: crack initiation

terial occurs [8]. Thereby, areas not involved in the crack propagation process do not reveal the dimple configuration [8] as shown in figure 8a. The fracture surfaces of the Irri S tips showed typical examples of mixed fracture modes with parts of fatigue failure and zones of skewed dimple fractures. The skewed dimple ruptures can develop from forced rupture. Afterwards, the starting point for a fracture can always be found at one of the edges. Throughout the ultrasonic activation, the starting point for the fracture progresses and reduces the diameter to an extent that leads to a more ductile skewed dimple fracture mode. Three out of 10 Irri S tips showed no fracture of the instruments after the application in the 3 mm radius of curvature canal. The length of the fractured segments was 7.9 mm in the canal with 2.5 mm radius of curvature and 7.2 mm in the canal with 3 mm radius of curvature. This region of the canal represents the area with the beginning of the curvature for a fully penetrated device. Manufacturer dependent material characteristics like machining grooves and scratches were detected on the whole surface of the instruments working part (Fig. 9 a–d; arrow). These are irregularities that serve as "stress-raisers" [41] and therefore as "initiators" of micro cracks. Fatigue failure only accounted for the Irri S tip, which might be explained with the material characteristics of these tips. The Irri S tip consists of chromium, iron and nickel (Fig. 4).

In contrast, ESI represents a NiTi-tip (Fig. 4). It has already been pointed out in the literature, that NiTi alloy appears highly flexible, elastic and works superior in curved canals [8, 19] compared to stainless steel instruments. A major disadvantage of this tip is the incompatibility of the tip and the intended device. It was not possible to attach the tip completely firm to the manufacturer's mounting, so all tested Endo Soft tips had a loose attachment during the experiments. This clearly affected the results as the energy transfer from the handpiece to the tip was impaired. Considering that ultrasonic irrigant activation may also result in uncontrolled removal of dentin [3], it is important to investigate the less aggressive sonic activation systems [12].

Eddy tips are made of polyamide and are longer (28 mm length) than the EndoActivator tips (21 mm/ 25 mm length), which are made of an unreinforced, low-viscosity acetal copolymer [12]. They showed no signs of fracture. However, the present study determined erosion of the instrument tips and levelled surface reliefs in both instruments. That raises the question of the whereabouts of the missing material. However, a rough tip surface could also provide advantages in terms of irrigant activation by enhancing the local streaming. According to manufacturer information, fractured Eddy tip fragments macroscopically visible move up in the canal with the irrigation solution. Nevertheless, under certain conditions it might be possible that microscopically visible material components remain in the ramified root canal system or are even transported with the irrigant flow to and beyond the apical region.

The present study showed that canals with small radii of curvature are difficult to manage with ultrasonic

irrigating activation in vitro. The Irri S tip broke more often than the sonic irrigation files. Consequently, Eddy seems like a promising system. Nevertheless, it is a relatively new device so case reports about treatment difficulties are missing.

Conclusively, the present study provides a basis for the establishment of further studies with additional parameters study by study in order to counteract the often-performed "trial and error"-study designs in medicine and dentistry. In this particular case, a follow-up study should implement artificial canals milled in bovine dentin with the curvature radii of the current study. However, this investigation enables a defined comparative assessment of different sonic and ultrasonic irrigation activation devices under completely standardized conditions.

Conclusions

An artificial and standardized root canal model was successfully introduced with different radii of curvature, based on evaluations of human molars, for a comparative assessment of different sonic and ultrasonic irrigant activation devices. For a predefined cyclic fatigue test, it was demonstrated that the investigated polymeric sonic and NiTi-ultrasonic irrigant activation devices did not fracture due to the combined bending deformation with additional dynamic stress. Only the stainless steel ultrasonic device Irri S showed fatigue failure in canals with a small radius of curvature. However, the newly implemented approach is a model system that does not represent a realistic reproduction of the clinical conditions during irrigation procedures performed by a dentist. Thus, direct extrapolation to a clinical situation must be exercised with caution and further studies with additional influencing parameters are necessary.

Conflicts of interest:

The authors declare that there is no conflict of interest within the meaning of the guidelines of the International Committee of Medical Journal Editors.

References

1. Ajuz NC, Armada L, Goncalves LS, Debelian G, Siqueira JF Jr: Glide path preparation in S-shaped canals with rotary pathfinding nickel-titanium instruments. J Endod 2013; 39: 534–537

2. Basmadjian-Charles CL, Farge P, Bourgeois DM, Lebrun T: Factors influencing the long-term results of endodontic treatment: a review of the literature. Int Dent J 2002; 52: 81–86

3. Boutsioukis C, Tzimpoulas N: Uncontrolled removal of dentin during in vitro ultrasonic irrigant activation. J Endod 2016; 42: 289–293

4. Burroughs JR, Bergeron BE, Roberts MD, Hagan JL, Himel VT: Shaping ability of three nickel-titanium endodontic file systems in simulated S-shaped root canals. J Endod 2012; 38: 1618–1621

5. Cameron JA: The use of 4 per cent sodium hypochlorite, with or without ultrasound, in cleansing of uninstrumented immature root canals; SEM study. Aust Dent J 1987; 32: 204–213

6. Card SJ, Sigurdsson A, Orstavik D, Trope M: The effectiveness of increased apical enlargement in reducing intracanal bacteria. J Endod 2002; 28: 779–783

7. Chandran KSR: Mechanical fatigue of polymers: a new approach to characterize the S-N behavior on the basis of macroscopic crack growth mechanism. Polymer 2016; 91: 222–238

8. Cheung GS, Peng B, Bian Z, Shen Y, Darvell BW: Defects in ProTaper S1 instruments after clinical use: fractographic examination. Int Endod J 2005; 38: 802–809

9. Collins JA: Failure of materials in mechanical design: analysis, prediction, prevention. Wiley, New York 1981

10. Collins JA: Failure of materials in mechanical design: analysis, prediction, prevention. Wiley, New York 1993

11. Committee AIH, Mills K: ASM Handbook. ASM International, 1987

12. Conde AJ, Estevez R, Lorono G, Valencia de Pablo O, Rossi-Fedele G, Cisneros R: Effect of sonic and ultrasonic activation on organic tissue dissolution from simulated grooves in root canals using sodium hypochlorite and EDTA. Int Endod J 2016; 50: 976–982

13. Cunningham WT, Martin H: A scanning electron microscope evaluation of root canal debridement with the endosonic ultrasonic synergistic system. Oral Surg Oral Med Oral Pathol 1982; 53: 527–531

14. Dannemann M, Kucher M, Kirsch J et al.: An approach for a mathematical description of human root canals by means of elementary parameters. J Endod 2017; 43: 536–543

15. de Gregorio C, Estevez R, Cisneros R, Heilborn C, Cohenca N: Effect of EDTA, sonic, and ultrasonic activation on the penetration of sodium hypochlorite into simulated lateral canals: an in vitro study. J Endod 2009; 35: 891–895

16. Desai P, Himel V: Comparative safety of various intracanal irrigation systems. J Endod 2009; 35: 545–549

17. Fariniuk LF, Baratto-Filho F, da Cruz-Filho AM, de Sousa-Neto MD: Histologic analysis of the cleaning capacity of mechanical endodontic instruments activated by the ENDOflash system. J Endod 2003; 29: 651–653

18. Ferreira RB, Alfredo E, Porto de Arruda M, Silva Sousa YT, Sousa-Neto MD: Histological analysis of the cleaning capacity of nickel-titanium rotary instrumentation with ultrasonic irrigation in root canals. Aust Endod J 2004; 30: 56–58

19. Glossen CR, Haller RH, Dove SB, del Rio CE: A comparison of root canal preparations using Ni-Ti hand, Ni-Ti engine-driven, and K-Flex endodontic instruments. J Endod 1995; 21: 146–151

20. Goodman A, Reader A, Beck M, Melfi R, Meyers W: An in vitro comparison of the efficacy of the step-back technique versus a step-back/ultrasonic technique in human mandibular molars. J Endod 1985; 11: 249–256

21. Gu LS, Ling JQ, Huang XY, Wei X, Xu Q: [A micro-computed tomographic study of the isthmus in the root canal system of mandibular first molar]. Zhonghua Kou Qiang Yi Xue Za Zhi 2009; 44: 11–14

22. Gulabivala K, Ng YL, Gilbertson M, Eames I: The fluid mechanics of root canal irrigation. Physiol Meas 2010; 31: R49–84

23. Gutarts R, Nusstein J, Reader A, Beck M: In vivo debridement efficacy of ultrasonic irrigation following hand-rotary instrumentation in human mandibular molars. J Endod 2005; 31: 166–170

24. Gutierrez JH, Garcia J: Microscopic and macroscopic investigation on results of mechanical preparation of root canals. Oral Surg Oral Med Oral Pathol 1968; 25: 108–116

25. Haga CS: Microscopic measurements of root canal preparations following instrumentation. J Br Endod Soc 1968; 2: 41–46

26. Hieawy A, Haapasalo M, Zhou H, Wang ZJ, Shen Y: Phase transformation behavior and resistance to bending and cyclic fatigue of ProTaper Gold and ProTaper Universal instruments. J Endod 2015; 41: 1134–1138

27. Kiefner P, Ban M, De-Deus G: Is the reciprocating movement per se able to improve the cyclic fatigue resistance of instruments? Int Endod J 2014; 47: 430–436

28. Kuhn G, Jordan L: Fatigue and mechanical properties of nickel-titanium endodontic instruments. J Endod 2002; 28: 716–720

29. Lee SJ, Wu MK, Wesselink PR: The effectiveness of syringe irrigation and ultrasonics to remove debris from simulated irregularities within prepared root canal walls. Int Endod J 2004; 37: 672–678

30. Lee SJ, Wu MK, Wesselink PR: The efficacy of ultrasonic irrigation to remove artificially placed dentine debris from different-sized simulated plastic root canals. Int Endod J 2004; 37: 607–612

31. Lumley PJ, Walmsley AD, Walton RE, Rippin JW: Cleaning of oval canals using ultrasonic or sonic instrumentation. J Endod 1993; 19: 453–457

32. McGuigan MB, Louca C, Duncan HF: Endodontic instrument fracture: causes and prevention. Br Dent J 2013; 214: 341–348

33. Metzler RS, Montgomery S: Effectiveness of ultrasonics and calcium hydroxide for the debridement of human mandibular molars. J Endod 1989; 15: 373–378

34. Nagy CD, Szabo J, Szabo J: A mathematically based classification of root canal curvatures on natural human teeth. J Endod 1995; 21: 557–560

35. Pedulla E, Lo Savio F, Boninelli S et al.: Torsional and cyclic fatigue resistance of a new nickel-titanium instrument manufactured by electrical discharge machining. J Endod 2016; 42: 156–159

36. Plumbridge WJ: Review: Fatigue-crack propagation in metallic and polymeric materials. Journal of Materials Science 1972; 7: 939–962

37. Pruett JP, Clement DJ, Carnes DL Jr: Cyclic fatigue testing of nickel-titanium endodontic instruments. J Endod 1997; 23: 77–85

38. Sabins RA, Johnson JD, Hellstein JW: A comparison of the cleaning efficacy of short-term sonic and ultrasonic passive irrigation after hand instrumentation in molar root canals. J Endod 2003; 29: 674–678

39. Sauer JA, Richardson GC: Fatigue of polymers. Int J Frac 1980; 16: 499–532

40. Schafer E, Diez C, Hoppe W, Tepel J: Roentgenographic investigation of frequency and degree of canal curvatures in human permanent teeth. J Endod 2002; 28: 211–216

41. Schijve J: Fatigue of structures and materials. Springer Netherlands, 2009

42. Schneider SW: A comparison of canal preparations in straight and curved root canals. Oral Surg Oral Med Oral Pathol 1971; 32: 271–275

43. Shuping GB, Orstavik D, Sigurdsson A, Trope M: Reduction of intracanal bacteria using nickel-titanium rotary instrumentation and various medications. J Endod 2000; 26: 751–755

44. Siqueira JF Jr, Rocas IN: Polymerase chain reaction-based analysis of microorganisms associated with failed endodontic treatment. Oral Surg Oral Med Oral Pathol Oral Radiol Endod 2004; 97: 85–94

45. Spoleti P, Siragusa M, Spoleti MJ: Bacteriological evaluation of passive ultrasonic activation. J Endod 2003; 29: 12–14

46. Svec TA, Harrison JW: Chemomechanical removal of pulpal and dentinal debris with sodium hypochlorite and hydrogen peroxide vs normal saline solution. J Endod 1977; 3: 49–53

47. Takemori MT: Polymer fatigue. Annual Review of Materials Science 1984; 14: 171–204

48. Topcuoglu HS, Topcuoglu G: Cyclic fatigue resistance of reciproc blue and reciproc files in an s-shaped canal. J Endod 2017; 43: 1679–1682

49. Walton RE: Histologic evaluation of different methods of enlarging the pulp canal space. J Endod 1976; 2: 304–311

50. Wanhill RJH, Galatolo R, Looije CEW: Fractographic and microstructural analysis of fatigue crack growth in a Ti-6Al-4V fan disc forging. International Journal of Fatigue 1989; 11: 407–416

51. Weber CD, McClanahan SB, Miller GA, Diener-West M, Johnson JD: The effect of passive ultrasonic activation of 2 % chlorhexidine or 5.25 % sodium hypochlorite irrigant on residual antimicrobial activity in root canals. J Endod 2003; 29: 562–564

52. Wolf TG, Paqué F, Zeller M, Willershausen B, Briseño-Marroquín B: Root canal morphology and configuration of 118 mandibular first molars by means of micro-computed tomography: an ex vivo study. J Endodont 2016; 42: 610–614

53. Wong R: Conventional endodontic failure and retreatment. Dent Clin North Am 2004; 48: 265–289

(Photo: BW-Foto, Dresden)

DR. JASMIN KIRSCH
Clinic of Operative Dentistry, Medical Faculty Carl Gustav Carus, TU Dresden
Fetscherstr. 74, D-01307 Dresden
Germany
Jasmin.Kirsch@uniklinikum-dresden.de